Millimeter-Wave Tiny Lens Antenna Employing U-Shaped Filter Arrays for 5G

Eugean Kim, Seung-Tae Ko, Young Ju Lee, and Jungsuek Oh

***Abstract*—This letter presents a 28-GHz compact antenna array that employs a U-Shaped thin lens where a low-profile 1 × 4 antenna array is used as a feed source. The letter demonstrates that the proposed three-dimensional (3-D) U-Shaped lens designed by phase-shifting spatial filter arrays enables more than 3 dB peak gain enhancement even at the distance of less than half of the wavelength from the feed antenna. The first design step is to employ unit cells having a stable insertion loss and phase shift against the incident angle of electromagnetic waves without the gain degradation caused by undesired cavity effects, which is a critical bottleneck at such a short distance. In addition to this, the total gain is further enhanced by creating a novel 3-D U-Shaped architecture, enabling an increase in the effective aperture size because the U-Shaped thin lens can capture the radiated fields over a broader range of incident angles compared to the prior flat lens, which is more effective at a closer distance. This letter demonstrates that the proposed approach can achieve higher than 3.8 dB enhancement in peak gain compared to the antenna without the U-Shaped lens when the phase offset (PO) is 0°. When the levels of the PO are 45°, 90°, and 135°, gain enhancements of 3.4, 3, and 2 dB are also achieved, respectively.**

***Index Terms*—Beam steering, compact range, lens antennas, millimeter-wave antenna arrays.**

I. Introduction

METASURFACES have received considerable attention owing to the advantages of gain enhancement and beam controllability [1]–[3]. Most of the lens antennas have electrically massive apertures or multisegment stacked structure [2], [3]. This configuration cannot be compatible with upcoming millimeter-wave 5G products requiring commercially available printed circuit board fabrication process. The distance between the antenna and the lens is typically much longer than the free-space wavelength ($=\lambda_0$). This prohibits this type of antenna from being applied for low-mass and compact wireless devices.

Manuscript received November 19, 2017; accepted December 7, 2017. Date of publication March 23, 2018; date of current version May 3, 2018. This work was supported in part by the Basic Science Research Program through the National Research Foundation of Korea (NRF) funded by the Ministry of Science, in part by the Information and Communications Technologies and Future Planning under Grant NRF-2015R1C1A1A01055487, and in part by the ICT R&D program of MSIP/IITP (2016-0-00130, Cloud-Based SW Platform Development for RF Design and EM Analysis). *(Corresponding author: Jungsuek Oh.)*

E. Kim is with the Department of Electronic Engineering, Inha University, Incheon 402-751, Korea (e-mail: tangy@inha.edu).

S.-T. Ko and Y. J. Lee are with Samsung Electronics, Suwon 16677, Korea (e-mail: seungtae.ko@samsung.com; youngju0302.lee@samsung.com).

J. Oh is with the Department of Electrical and Computer Engineering, Seoul National University, Seoul 08826, Korea (e-mail: jungsuek@snu.ac.kr).

Digital Object Identifier 10.1109/LAWP.2018.2819022

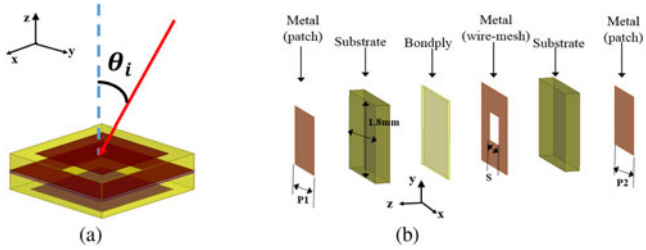

Fig. 1. (a) Drawings of the incident angle on a unit cell and (b) exploded view of a bandpass unit cell.

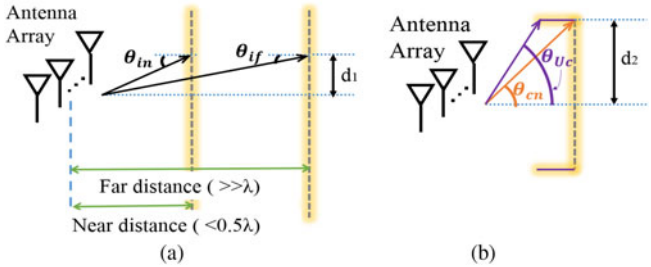

Fig. 2. Drawings of incident angles on (a) flat aperture at near and far, and (b) U-shaped aperture.

The earlier approaches rely on utilization of different phase delays that are obtained by different topologies of the unit cells but typically assuming that the effects of oblique wave incidence on the unit cell are negligible [1]. The incident angle θ_i is formed by the direction vector of the incident wave and a vector perpendicular to the lens plane, as shown in Fig. 1(a). The incident angle is two-dimensionally different in respect of the position of the unit cell, which affects both the phase shift and the insertion loss of the unit cell at different levels. In Fig. 2(a), θ_{in}, which is the incident angle at the near distance from the antenna, is much greater than θ_{if}, which is the incident angle at the far distance from the antenna. Furthermore, it is found that once the flat aperture at the near distance is bent, the angular coverage ($=\theta_{Uc}$) capturing the radiated fields at the near distance ($=\theta_{cn}$) is effectively increased in Fig. 2(b).

In this letter, the first design goal is to achieve the gain enhancement by utilizing a small-aperture two-dimensional (2-D) flat lens as a collimator in the near distance from a feed array. The second goal is to realize effective utilization of a small volume by designing a U-Shaped structure, achieving an increase in effective aperture size. The third goal is to devise a design technique to acquire a moderate angular coverage

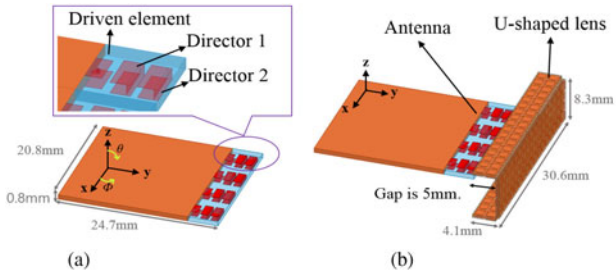

Fig. 3. (a) 1 × 4 feed antenna array and (b) U-Shaped lens antenna.

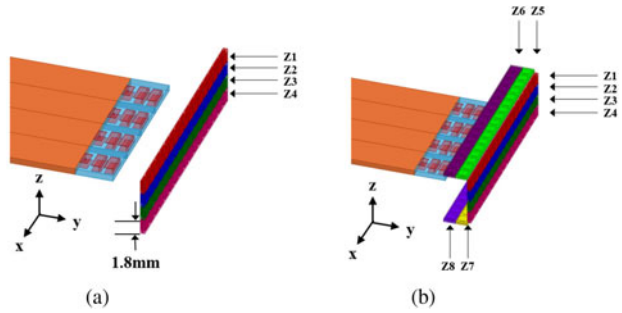

Fig. 4. Separated zones of (a) the flat lenses and (b) the U-Shaped lens.

along the azimuthal axis, which is essential for modern wireless communications.

II. Lens Design

A tiny U-Shaped thin lens adjacent to a small-size antenna is proposed to boost the antenna gain while maintaining the angular coverage along the azimuthal axis. A 1 × 4 antenna array producing θ-polarized radiated fields is designed to have the dimensions of 24.7 mm (= lateral dimension along the *y*-axis) by 20.8 mm (= lateral dimension along the *x*-axis) by 0.8 mm (= profile) at 28 GHz, as shown in Fig. 3(a). A single element in the antenna array consists of a driven element and two parasitic directors, as shown in Fig. 3(a) [4]. The driven element exciting the directors comprises top and bottom patch plates where the top plate is connected to a feedline while the bottom plate is connected to the ground. The medium between the two plates is filled with FR4 whose dielectric constant is 4.4 and whose loss tangent is 0.02. The antenna has radiation characteristics of vertical polarization coupled by parallel metallic plate of driven element. Antenna directivity is enhanced in the direction along which the two directors are arranged. The directors also include the top and the bottom plates, and the two plates are physically connected to each other through numerous shorting vias. Fig. 3(a) shows a simplified version of the director in which the vias are replaced by a rectangular sheet to save the computational time.

In feed network, phase shifters are utilized instead of the switches, and this can achieve electronically quasi-continuous beam steering with minimum scan loss, while use of multi-stage switches in the millimeter-wave frequencies and such high frequencies may increase feed losses significantly, which may hamper an efficient system design.

The lens is placed close to the antenna array at a distance of 5 mm, which is half of the wavelength at 28 GHz. The U-Shaped lens is designed to have the dimensions of 4.1 mm × 30.6 mm × 8.3 mm, as shown in Fig. 3(b). The lateral dimension of a single unit cell in the lens is 1.8 mm. The unit cell consists of conductive layers of copper having the shapes of a patch and a wire mesh, and substrate layers of Rogers 6010 whose dielectric constant is 10.2 and whose loss tangent is 0.0023. The substrate layers are sandwiched by the conductive layers, as shown in Fig. 1(b). The thicknesses of the Rogers 6010 and the bondply are 0.25 and 0.04 mm, respectively. Different phase delays are produced by changing each metal layer's dimension parameters P1, P2 as patch sizes, and *S* as slot size of the wire mesh. The unit cells are designed to have a wide tunable range of the phase shift within the 1 dB of insertion loss. The design parameters, phase shifts, and insertion losses of the unit cells filling each zone in the proposed lens in Fig. 4(a) and (b) are listed in Tables I and II, respectively. In the simulation procedure, the transmission and phase of S_{21} is extracted utilizing the periodic boundary conditions applied along the *yz* plane and *zx* plane [5].

TABLE I
Dimension Parameters, Phase Shift, and Insertion Loss of Unit Cells With Various Incident Angles and Selected Unit Cell Number for Each Zone of Flat Lens 1 and Flat Lens 2

	Zone	UC#	P1	P2	S	Incident Angle(°)	Insertion Loss(dB)	Phase(°)
Flat lens 1	Z1,Z4	1	1.45	1.375	1.15	0	0.25	-149
						30	0.24	-145
						60	0.2	-138
	Z2,Z3	2	1.35	1.35	0.65	0	0.69	-92
						30	0.77	-88
						60	2.13	-88
Flat lens 2	Z1,Z4	1	1.45	1.375	1.15	0	0.25	-149
						30	0.24	-145
						60	0.2	-138
	Z2,Z3	3	1.3	1.3	0.8	0	1.04	-90
						30	0.82	-87
						60	0.62	-93

TABLE II
Dimension Parameters, Phase Shift, and Insertion Loss of the Unit Cells With Various Incident Angles and Selected Unit Cell Number for Each Zone of the U-Shaped Lens

	Zone	UC#	P1	P2	S	Incident Angle(°)	Insertion Loss(dB)	Phase(°)
U-shaped Lens	Z1,Z4	1	1.45	1.375	1.15	0	0.25	-149
						30	0.24	-145
						60	0.2	-138
	Z2,Z3	3	1.3	1.3	0.8	0	1.04	-90
						30	0.82	-87
						60	0.62	-93
	Z5,Z7	4	1.4	1.3	0.8	0	0.74	-108
						30	0.55	-106
						60	0.37	-101
	Z6,Z8	5	1.25	1.25	0.8	0	0.72	-69
						30	0.55	-68
						60	0.63	-68

A. Limit of Conventional Designs

In the conventional approach to design millimeter-wave thin lenses by utilizing spatial filter arrays, a design procedure to determine the required values of the phase shift by the unit cells on lens aperture is as follows:

Step 1: Extract the degree of phase shift from phase information considering the polarization vector, which is determined to be tangential to the lens plane.

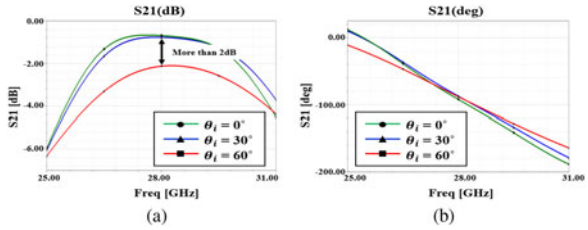

Fig. 5. (a) Magnitude and (b) phase of S_{21} of the prior unit cells versus different incident angles of 0°, 30°, and 60°.

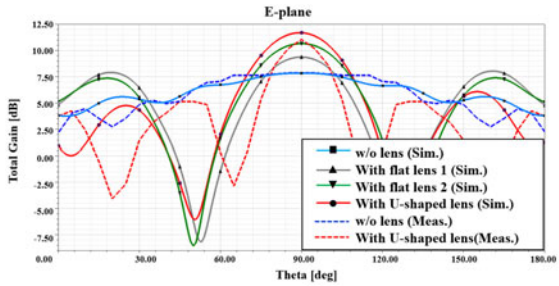

Fig. 6. Simulated and measured results on *E*-plane.

Step 2: Extract the needed phase shift of the lens from the phase information.

Step 3: Divide a lens aperture into the zones along the direction of beam steering.

Step 4: Determine the needed phase variations along the elevation of the 2-D lens aperture and apply different levels of a tapering in the phase variation until maximum gain corresponding to vertical polarization that is co-polarization in this letter is acquired.

In Step 3, to avoid the radiation pattern distortion caused by the erratic phase shift occurring on the lens with beam steering on the *xy* plane (=azimuthal plane), the same type of unit cell is arranged along the *x*-axis while different types of unit cells are arranged along the *z*-axis for a beam narrowing, enabling gain enhancement, as depicted in Fig. 4(a).

The variation of S_{21} indicating the transmittance through the lens is investigated by changing the incident angle. In most of the prior study, unit cell simulations are performed under the assumption of wave incidence normal to the lens plane because this type of the lens has long been designed to operate at the distance of multiple wavelengths from the feed antenna. On the other hand, Fig. 5 suggests that S_{21} of the lens is significantly affected by the incident angle at the near distance, and variation in insertion loss is much higher than that in phase shift. In the case of this selected unit cell (= UC2), this lens suffers from high insertion loss at the incident angle of 60°. Therefore, selecting unit cells whose insertion loss is independent of the incident angle is important for near-field lens design. In order to prove the effectiveness of this statement at a very close distance, two different types of lenses, as shown in Fig. 4(a), were designed, denoted by "Flat lens 1" and "Flat lens 2." In the two lenses, same types of unit cells are used for zones Z1 and Z4, while different types of unit cells having different responses against the incident angle, are used for Z2 and Z3. For the two lenses, the responses of insertion loss are quite different depending on the incident angle, while their phase responses are similar. In Fig. 2(a), at a fixed distance (= d_1) from the center of the lens aperture, θ_{in} is larger than θ_{if}, indicating the aforementioned effects of the incident angle at near distances.

The proposed lens antennas are simulated by using a full-wave electromagnetics solver, Ansys HFSS. Both of the antennas employing "Flat lens 1" and "Flat lens 2" in Table I improve the peak gain of the main beam compared to the case of "Without lens (denoted by w/o lens)" by 1.5 and 2.8 dB, respectively. However, "Flat lens 2" achieves a 1.3 dB higher peak gain enhancement than "Flat lens 1." This confirms that a small difference in the distribution of the unit cells can cause an approximately 1.3 dB gain degradation for a tiny and nearby radiating aperture. Fig. 6 shows the gain in the *yz* plane (= *E*-plane) of simulated radiation patterns of the two flat lenses. The aforementioned effects of the incident angle on the lens gain are investigated under the conditions of a short distance of 5 mm (= $0.5\lambda_0$) and a profile of the whole structure (= 8.3 mm).

TABLE III
COMPARISON OF SIMULATED AND MEASURED PEAK GAINS FOR THE CASES OF "WITH U-SHAPED LENS" AND "WITHOUT U-SHAPED LENS" WHEN PO IS 0° AND 90°

Phase Offset(°)	Lens	Simulated Gain enhancement by lens(dB)	Simulated Tilted angle(°)	Measured Gain enhancement by lens(dB)	Measured Tilted angle(°)
0	Without	3.83	0	3.8	3
	With		0		-1
90	Without	3.01	27	2.05	34
	With		23		31

B. Novel Approach by Employing U-Shaped Structure

The final structure of the proposed lens, the U-Shaped thin lens, is realized by designing the upper and lower parts extended and bent from the aforementioned "Flat lens 2." They are zones Z5, Z6, Z7, and Z8, as depicted in Fig. 4(b). This U-Shaped architecture can guide radiating waves at an extended coverage on the *yz* plane in a fixed distance, as described in Fig. 2(b).

The needed phase shifts for the bent upper and lower parts are derived by the same procedure from Steps 1 to 3, as explained in Section II-A. A polarization vector to extract the phase of the propagating rays is selected to be tangential to the *xy* plane in Step 4. However, unlike the flat structure, the added upper and lower apertures are arranged to be parallel to the direction of the main beam, while the conventional lens aperture is perpendicular to the direction of the main beam. Therefore, the physical area of the aperture is not increased in terms of the direction of the main beam. Unit cell information regarding the added upper and lower parts is listed in Table II.

The design of the U-Shaped thin lens enables a further gain enhancement of 1 dB, compared to the proposed "Flat lens 2." Comparisons in total gain among the discussed lenses are shown in the *yz* plane (= *E*-plane) of Fig. 6. The simulated radiation patterns of the antennas are shown in the range of 0° to 180° in terms of θ. To examine the beam steering capability of the proposed antenna using the three-dimensional (3-D) U-Shaped thin lens, the aforementioned antennas are simulated and measured for the different levels of the phase offset (PO). Fig. 7 shows the simulated radiation patterns for the cases of "With U-Shaped lens" and "Without U-Shaped lens" when the PO is 0°, 45°, 90°, and 135°. Table III shows the lens gain, which is the difference in gain between the cases "With U-Shaped lens" and "Without U-Shaped lens" as a function of PO related to the

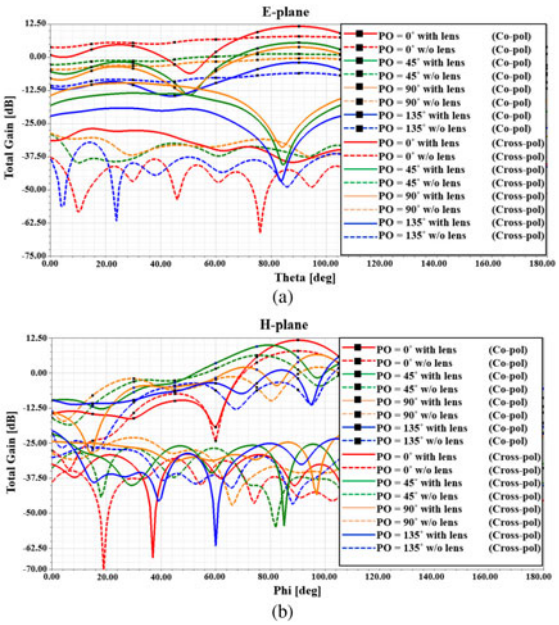

Fig. 7. Comparison between without and with the U-Shaped lens in terms of beam steering on (a) *E*-plane and (b) *H*-plane.

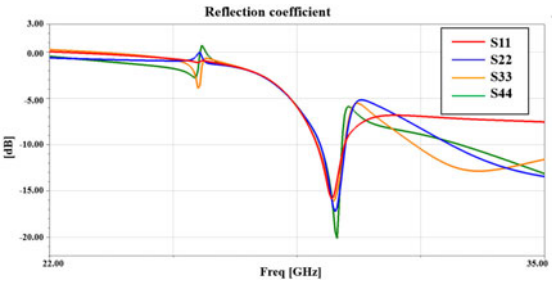

Fig. 8. Magnitude of reflection coefficient of the U-Shaped lens antenna.

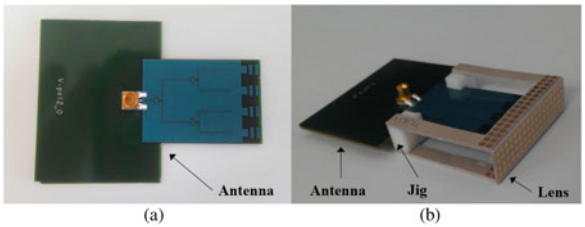

Fig. 9. Fabricated samples of (a) feed antenna array without U-Shaped lens and (b) proposed antenna with U-Shaped thin lens.

tilted angle of the main beam. The results confirm that utilization of the unit cells having the uniform topology along the *x*-axis prevents an increase in scan loss related to the angular coverage as intended. The aperture efficiency is calculated as 52%, and the total efficiency is 43% where the total efficiency is defined as a multiplication of the aperture efficiency of 52% and the antenna efficiency of 82%. A resonant frequency of about 28 GHz is confirmed by the reflection coefficient in Fig. 8.

III. Fabricated Samples and Measurement Setup

For the cases "Without U-Shaped lens" and "With U-Shaped lens," fabricated samples are shown in Fig. 9(a) and (b). The lens described in Fig. 9(b) is combined with a jig that fixes the lens against the antenna accurately. The jig holds both ends of the U-Shaped lens so as not to cause undesired reflections from the jig.

A measurement setup is established in an anechoic chamber. In this setup, a standard horn antenna, as a receive antenna, is connected to one port of a vector network analyzer, and the other port is connected to the lens antenna. Measured results are acquired in the presence and absence of the proposed lens corresponding to the aforementioned cases "Without U-Shaped lens" and "With U-Shaped lens," respectively. The measurement results confirm that the proposed lens antenna can achieve up to 3.8 dB enhancement in peak gain, as observed in Fig. 6. The lens antenna still provides 2 dB gain enhancement with a beam steering scenario where PO is 90°, as shown in Fig. 10.

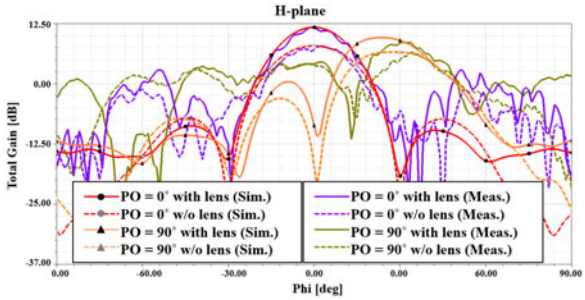

Fig. 10. Comparison of measurement and simulation result about antenna without and with the U-Shaped lens for beam steering of *H*-plane.

IV. Conclusion

This letter introduces a tiny lens design employing the unit cells independent of the incident angle and a U-Shaped topology at a very close distance ($<0.5\lambda_0$) from the antenna array operating at 28 GHz. First, for such a short distance, the resulting gain enhancement factor is discussed from a sophisticated consideration of the incident angle. Second, it is demonstrated that employment of the proposed U-Shaped thin lens enables a further gain enhancement by increasing the effective aperture size in the direction of the main beam. In addition, it should be noted that the proposed tiny lens antenna is designed to maintain angular coverage along the *xy* plane, which is essential for modern, low-profile 5G applications demanding efficient end-fire radiation.

References

[1] J. Oh, "Millimeter wave short-focus thin lens employing disparate filter arrays," *IEEE Antennas Wireless Propag. Lett.*, vol. 15, pp. 1446–1449, 2016.

[2] T. K. Nguyen *et al.*, "Design of a low-profile, high-gain Fabry–Perot cavity antenna for ku-band applications," *J. Electromagn. Eng. Sci.*, vol. 14, no. 3, pp. 306–313, Sep. 2014.

[3] D. Kim, "A sub-wavelength focusing lens composed of a dual-plate metamaterial providing a negative refractive index," *J. Electromagn. Eng. Sci.*, vol. 12, no. 1, pp. 26–31, Mar. 2012.

[4] W. Hong *et al.*, "Compact 28 GHz antenna array with full polarization flexibility under yaw, pitch, roll motions," in *Proc. 2015 9th Eur. Conf. Antennas Propag.*, Apr. 2015, pp. 1–3.

[5] J. Oh, "Millimeter wave thin lens employing mixed-order elliptic filter arrays," *IEEE Trans. Antennas Propag.*, vol. 64, no. 7, Jul. 2016, pp. 3222–3227.